Innovative Optoelectronic Approaches to Biomolecular Analysis with Arrays of Silicon Devices

C. Guiducci[1], C. Stagni[1], M. Brocchi[1], M. Lanzoni[1], B. Riccò[1], A. Nascetti[2], D. Caputo[2], and A. De Cesare[2]

[1] DEIS University of Bologna, Viale Risorgimento 2, 40136 Bologna-ITALY, cguiducci@deis.unibo.it

[2] DIE University of Rome "La Sapienza", Via Eudossiana 18, 00184 Roma-ITALY decesare@die.uniroma1.it

Abstract. This paper intends to provide a brief survey of the most advanced implementations of molecular analysis tools based on microtechnologies and to discuss a new approach for the development of integrated molecular analysis. The technique presented hereafter combine a label-free method for molecular characterization based on UV absorbance and two technologies of silicon photodetectors addressed to fulfill the requirements of different applications.

1 Introduction

Microtechnologies play a crucial role in the development of innovative low-cost and mass-produced assays for bio-sensing and bio-interactive purposes. In some areas, their use in the development of bio-interactive systems is already well-established. For instance, microsystems for in-body drug delivery and passive silica chip (or slides) for high-parallel molecular analysis are among the most important innovations.

The advantages derived by the use of advanced devices can be summarized as follows:

- The miniaturization of the reaction sites and cells allows the use of a reduced amount of sample and reagents.
- The miniaturization of the measurement system leads to portability and a higher signal-to-noise ratio.
- The possibility to implement high-parallel analysis tools increases of orders of magnitude the speed of analysis.
- The integration of mechanical and fluidic functions for sample handling, delivery, mixing, purification, separation, and amplification leads to stand-alone and easy-to-use devices. In case of miniaturized handling, volumes are often in the nanoliter to picoliter range rather than the microliter range needed for conventional experiments.
- The possibility to provide low-cost and mass-produced assays by batch production.

Please use the following format when citing this chapter:

Guiducci, C., Stagni, C., Brocchi, M., Lanzoni, M., Riccò, B., Nascetti, A., Caputo, D. and De Cesare, A., 2007, in IFIP International Federation for Information Processing, Volume 249, VLSI-SoC: Research Trends in VLSI and Systems on Chip, eds. De Micheli, G., Mir, S., Reis, R., (Boston: Springer), pp. 37–53

- The generation of electrical read-out by the integration of electronic sensors allows the use of microelectronic circuits available for electrical signal conditioning, amplification, filtering, modulation, and transmission.
- The sensing performance can be increased by using high-sensitive electron devices.

The following section provide a survey of some of the most interesting implementations of molecular analysis assays based on advanced technologies, from the point of view of sample handling functions (Sect. 2.1), of electronic devices for parallel molecular detection (Sect. 2.2) and of micromachining implementations for molecular analysis (Sect. 2.3). In Sect. 3 we present the state-of-the-art of integrated optical sensing of molecular reactions and we describe the new approaches we tested based on UV absorbance.

2 Microtechnologies for Biomolecular Analysis

2.1 Total Analysis Systems on a Chip

Integrated microfluidics may be made of plastic, glass, quartz, or silicon. Bulk and surface micromachining performed with sophisticated etching, patterning and deposition techniques are at the basis of channels implementation.

One of the most relevant microfabricated implementation on chip is the Polymerase Chain Reaction (PCR) molecular amplification. This approach has been widely investigated exploiting the good properties of thermal conductivity of silicon and its ability to easily integrate thermal resistances [1],[2],[3].

A large number of basic fluidic components have been assembled in different ways to perform various other chemical process. Many of these are based on electrokinetic transport principles, and include valves, mixing structures, chemical reactors, and chemical separation channels. In addition, chemical separation mechanisms have been miniaturized, including gel electrophoresis, solvent programmed chromatography, isoelectric focusing, isotachophoresis and two-dimensional separations based on liquid chromatography and free-solution electrophoresis. Surface interactions have been exploited for solid-phase extraction to process samples for hybridization of target DNA molecules, and nanoliter-scale reactors have been demonstrated for continuous flow, stopped flow, and thermal cycling reactions [4],[5],[6].

2.2 Electronic Circuits for Bio-sensing Transduction and Processing

Printed Circuit Technology for DNA Detection An electrical-based DNA analysis system has been developed by Motorola (Clinical Microsensors Division). It is based on an electronic instrumentation and on disposable chips implemented with printed circuit board technology. Few dozens of gold electrodes of 250 μm are defined on the board where DNA capture probes are immobilized by a self-assembled monolayer technology. Target DNA molecules are detected

by specific probes in a first stage. Then, a second probe, which hosts an electroactive label, is used to generate a current signal on the corresponding site [7]. The electronic instrumentation performs alternating current voltammetry on the disposable chip and identifies the site where specific DNA hybridization has occurred.

An Active Chip for Direct DNA Detection Recently, Infineon Technologies has developed two generations of fully-electronic sensor arrays for DNA detection based on CMOS technology.

The chips are implemented in $0.5\,\mu m$ CMOS process extended with additional process steps meant to form gold electrodes on the top. The electrodes are connected to the integrated circuits by means of vias of composite structures of different metals. A single sensing site array is made of two interdigitated gold electrodes arranged within a circular surface of down to $100\,\mu m$ diameter. The spacing between the fingers and their width is $1\,\mu m$. Single-stranded DNA probe molecules are deposited by microspotting technology and immobilized on the gold surface by covalent AU-S bonds. After immobilization, a liquid sample containing the target molecules to be detected is applied to the surface of the whole chip and, in case of matching sequences, an hybridization reaction occurs capturing permanently the targets.

In the first chip – a 16×8 sensor array – an enzyme label (alkaline phosphatase) is beforehand bound to the targets molecules in order to generate an electrochemical signal after the hybridization reaction. The electrochemical activity of the enzyme is detected by applying a suitable chemical substance (p-aminophenyl-phosphate) and performing redox-cycling measurements. The magnitude of the redox current between the finger electrodes depends on the amount of detected targets. The circuits within each position allow to detect sensor currents in a range between $10^{-12}\,A$ and $10^{-7}\,A$ [8].

In a further chip realization, a label-free detection technique has been successfully applied. The detection principle relies on the interface capacitance change led by the hybridization reaction. Indeed, the interface capacitance depends on the configuration of the layer of ions in the vicinity of the electrodes which is affected by the molecules immobilized on the gold surface. The electrodes which captured target molecules ad thus host double-stranded molecules, exhibit a capacitance 20% smaller than the one of the other electrodes. Input/output signals are both analog and digital but the output is fully digital, as CMOS circuits placed below each of the 128 interdigitated electrode perform internally capacitance measurement and analog-to-digital conversion by mixed signal. The conversion is performed in parallel and results are multiplexed on the output using the address signals [9].

2.3 Micromachining for High-sensitive Structures

Microcantilevers for Molecular Mass Sensing Surface and bulk micromachining techniques may help with providing innovative solutions for molecular

sensing at the microscale level. Silicon nitride cantilevers have been tested for sensing of molecular binding events. The detection principle is based on the detection of mass changes or on the surface stress change at the cantilever by measuring the change of the resonant frequency or of the bending, respectively. Both label-free and label-mediated techniques have been successfully employed. The recent discovery of the origin of nanomechanical motion generated by DNA hybridization and proteinligand binding provided some insight into the specificity of the technique. DNA hybridization detection, including accurate positive/negative detection of one base pair mismatches have been reported by [10] and [11].

Porous Materials Porous materials are suitable structures for surface sensing techniques as they provide a high surface/volume ratio. Moreover, this technology is meant to create inexpensive devices. High surface areas provide a mechanism to achieve detection sensitivities that are in the range of parts per billion on a short time scale.

DNA hybridization has been detected in a porous silicon media by the interferometric Fabry-Perot technique [12]. Other powerful optical techniques, like the super-prism phenomenon are also under investigation [13].

3 Optical Sensing of Molecular Reactions

Glass arrays for molecular analysis are widely employed in fields like drug discovery, genetic research and medical diagnostics (at the research level). Each site can recognize and capture specifically an identifying part of a gene, a RNA strand or a protein.

At present, these detection systems need a preparation step of optical functionalization of target biomolecules (labeling) and the use of high-cost scanning fluorescence detectors. They relies on the quantification and/or the localization of target biomolecules by means of fluorescent labels. The slides host two-dimensional arrays of small sites (from $20\,\mu m^2$ to $400\,\mu m^2$), on which different molecular probes are immobilized.

Recent works witness the effort of developing arrays of solid state optical devices able to detect on-site the emitted light of the fluorescent labels. The interest in integrated detectors is led by the demand for low-cost devices, to be employed even outside specialized laboratories and addressed to mass-production. These photodiodes arrays are meant both to be coupled with glass structures [14],[15],[16],[17], and to become active sensing substrates for the molecular-spotted arrays [18],[19],[20]. In the latter approach, probes may be spotted directly on the top of the chip by chemically modifying the silicon dioxide passivation. Nevertheless, the integration of optoelectronic detection on existing fluorescence microarrays is still far to be achieved [21], being the reason the non trivial design issues due to the need for integrated filters to screen the excitation light. Moreover, fluorescent labels have been demonstrated to be quite unreliable employed in common scanning procedures [22].

We recently considered a different sensing approach which relies on the intrinsic optical absorbance of biomolecules in the far-UV range. The absorption properties of polynucleotide molecules (DNA and RNA) are highly specific, well-characterized and able to provide quantitative information as well as molecular composition indications [23]. UV absorbance is widely employed to characterize volume samples and even molecular layers [24],[25],[26].

Here, we present some innovative approaches based on the measurement of UV absorbance for DNA strands quantification and detection, suitable for fully-integrated analysis systems.

A system integration perspective must start from the analysis of the existing array surfaces and their needs in terms of densities according to the different applications. At present, existing arrays differs for both dimensions and density of molecular spots per square centimeters. The use of a single chip of mono-crystalline silicon seems to be the natural electronic evolution of quartz high-throughput, high-density microarrays, like the one created by Affymetrix (surface $1.2\,cm^2$). These passive chips, implemented with photolithographic techniques are able to test a whole genome in parallel, with densities of one million sites per square centimeter [27].

Nevertheless, low or medium density array (from ten sites [28],[29] to forty thousand sites [30]) - suitable for analysis targeted to a restricted number of genes - are usually spotted on very large areas (several square centimeters). As a result, to provide on site optoelectronic detection a different technology should be considered.

In what follows, the paper presents different technologies for UV-based molecular detection that are suitable to different applications. In specific, Sect. 3.1 concerns the use of amorphous silicon p-i-n junctions in the measurements of extremely low concentrations of molecules and the suitability of these devices for surface detection of long DNA molecules. Section 3.2 presents the use of UV high-sensitive floating gate memories implemented in CMOS technology for the measurements of molecular absorbance. This technology allows very dense implementations and the integration of additional circuitry for processing of large amount of data. In Sect. 4 are drawn some conclusions.

3.1 Amorphous Silicon P-I-N Junctions

Amorphous silicon technology is particularly suitable for microsystem implementations of analysis tools. It involves low-cost and low-temperature processes, thus, it is suitable to be integrated directly on glass or plastic microfluidics. Amorphous silicon photodetectors are well-known to be high-sensitive devices which can be tuned to be specific to a narrow range of wavelengths [31]. Recently, they have been employed in integrated system for fluorescence detection on molecular assays [15],[20].

Here, we present experimental results of molecular characterization obtained by high-sensitive p-i-n structures of composite amorphous silicon. We describe two employments of such devices, namely the characterization of low-molecular

concentrations (see Sect. 3.1 and the use of photodetectors coupled with molecular sensing spots (see Sect. 3.1).

Device We describe the design choices which aim at providing very high-sensitive UV detectors. In the attempt to make inexpensive and compact analysis systems there the use of low-molecular concentrations and of low UV radiation intensity levels are needed.

These devices, already presented in [32], are n-type amorphous silicon/intrinsic amorphous silicon/p-type amorphous silicon carbide (a-SiC:H) stacked structures (n-i-p) grown by Plasma Enhanced Chemical Vapor Deposition (PECVD) on a glass substrate covered by Cr/Al/Cr metal layers (top and front view are shown in Fig. 1). The top contact is a Al/Cr metal grid, whose spacing is optimized for charge collection by taking into account the conductivity of the underlying p-layer. The p-layer is the active zone of the device. In order to ensure good collection efficiency, thus sensitivity, the p-layer thickness has to be less than the electron diffusion length in the p-doped layer and more than the distance needed to generate the built-in potential. A good trade-off between these two competitive requirements is obtained by setting the thickness to $5\,nm$. The i-layer composition and thickness are determined to keep the dark current as low as possible. As a first step, this specification can be met by using hydrogenated amorphous silicon for the intrinsic layer; this allows to reduce the defect density in the i-region, hence the contribution to the inverse saturation current due to thermal generation. The optimum value of the thickness is found to be $150\,nm$, which allows to achieve the minimum of the inverse saturation current around $5 \times 10^{-11}\,A/cm^2$ at small reverse bias. The part of the device under the grid is $2 \times 2\,mm^2$. The metal grid of the device has a pitch of $200\,\mu m$ and the width of the fingers is $50\,\mu m$. The responsivity measured is $45\,mA/W$. The quantum yield is around 0.15 for wavelengths below $300\,nm$.

Method The UV optical absorbance A_M of a molecular sample is given by the Lambert-Beer law :

$$A_M = -Log(Int_M/Int_0) \tag{1}$$

where Int_0 is the intensity of light transmitted to the detectors through a reference sample, (*i.e.* in absence of absorbing molecules) and Int_M the intensity transmitted by an equivalent sample containing molecules. The current flowing through the p-i-n junction and the intensity incident on the detectors being proportional, it is possible to substitute the ratio between the intensities with the ratio between the detector currents I_0 and I_M:

$$A_M = -Log(I_M/I_0) \tag{2}$$

In order to evaluate the characteristics of an optimized device, it is very important to point out the role of the absorbance of the reference sample. As it will be described in Sect. 3.1, when dealing with microarrays of sensing sites

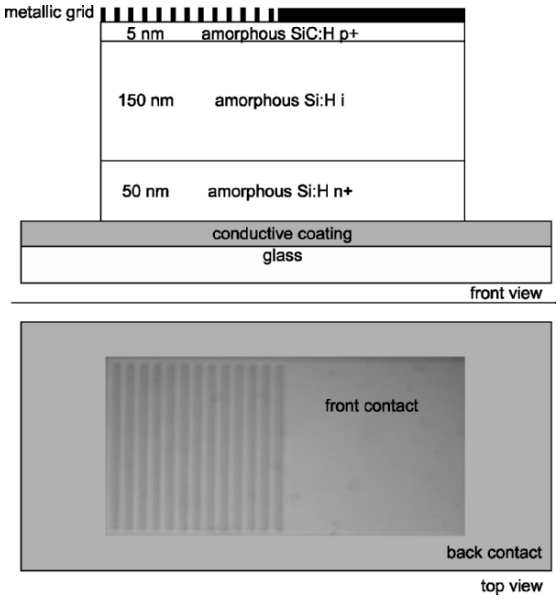

Fig. 1. Front view and top view of the amorphous silicon photodetector. The device surface is $2 \times 4\,mm^2$

the reference absorbance is the one of the sensing site prior to target molecules binding (it is due to the quartz substrate, the linkers and the probes). The resolution of the system (or the minimum detectable absorbance of the captured target molecules), depends on the current working point, defined by the absorbance of the sensing site before molecular recognition reaction. In fact, being eI the absolute error on the photocurrent, a variation of absorbance can be detected if the corresponding variation of the photocurrent is twice the noise current ($6dB\,SNR$). The minimum variation of the current corresponding to the sensing site I_0 that can be detected is $2 \cdot eI$. It follows that:

$$minA_M(I_0) = -Log((I_0 - 2 \cdot eI)/I_0) \tag{3}$$

where $minA_M$ is the minimum detectable absorbance of captured layer on this sensing site. As I_0 is a function of the absorbance of the sensing site A_0:

$$A_0 = -Log(I_0/I_{void}) \tag{4}$$

the function $minA_M(A_0)$ can be derived. I_{void} is the photocurrent sensor in absence of the quartz slide and corresponds to $I_{void} = P_0 \cdot R$, where P_0 is the power of the light source and R is the responsivity.

Setup The sensitivity of UV photodetectors has been evaluated by the optical setup drawn in Fig. 2. The light, generated by a mercury lamp, has been filtered

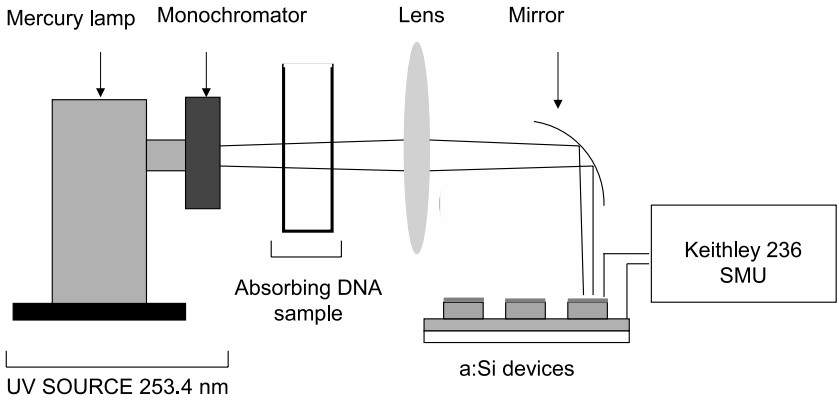

Fig. 2. Optical setup employed in the measurement of DNA molecular samples.

by a *Yobin-Yvon SPEXH10* monochromator. Devices has been tested at a wavelength of 253.4 nm which is located in the absorption peak region of nucleotides (maximum: 260 nm) [23]. The incident power on the sensor is 0.35 μW. UV optics (a lens and a mirror) have been used for beam collimation and focusing while a *Keithley 236 Source Measure Unit* has been employed for the measurement of the a-Si:H sensor current. To validate the UV approach to DNA microarrays, we have compared the absorbance of sensing sites where target DNA binding has and has not taken place, respectively. Bio-functionalized quartz slides have been aligned with the photodetectors (Fig. 3).

High-sensitive molecular sample characterization The sensitivity of the detectors has been investigated by measuring the absorbance of molecules in solution down to very low concentrations. Short sequences of the single-stranded form of DNA have been selected: $30-mer$ $5'-$gat cat cta cgc cgg acc cgg gca tcg tgg$-3'$ (MW 7669 $g/mole$, extinction coefficient 260700 $L/mole \cdot cm$). The molecules have been diluted to different concentrations into a TAE Mg^{++} buffer and placed in a quartz container.

The DNA absorbance (A_{DNA}) has been calculated by using 2 where the reference sample was a buffer solution of TAE Mg^{++} at room temperature. The short term variability of the mercury lamp intensity has been monitored by measurements of the white field. In Fig. 4 the calculated absorbances for different concentrations (following from 2) have been compared to their nominal value. A good linearity can be observed down to 3×10^{-4} absorbance. Figure 2 shows the setup corresponding to the characterization of molecular samples in solution Sect. 3.1.

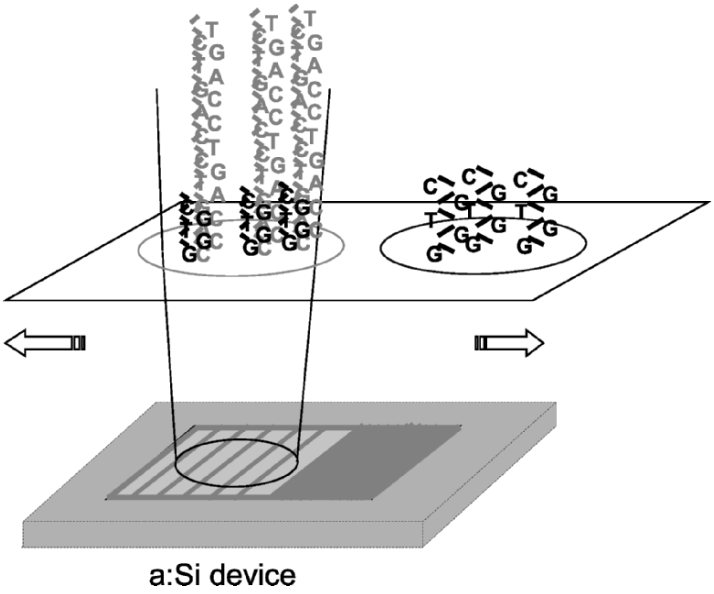

Fig. 3. A site with probes and captured long target sequences has been aligned with the exposed part of the detector. The other site has been aligned on the sensor by a shift of the slide.

Target Molecules Detection on Surface Sites The ability given by a:Si technology to deposit large area arrays allows the implementation of detectors slides meant to integrate most existing DNA microarrays the way they are (for example low/medium density array spotted on standard microscope slides). To demonstrate the viability of the UV approach to DNA microarrays, we detected a layer of captured target molecules on sensing sites with UV a:Si detectors. Sensing sites hosted short probe strands which could capture specifically long strands of target molecules thanks to the complementarity between their sequence and a part of the target.

Device The target molecule is pBR322 linearized with PvuII, a commonly used plasmid cloning vector of 4361 base length (extinction coefficient at $260\,nm$: $4 \times 10^7\,l/mole \cdot cm$). The sites have been exposed to unlabeled target molecules at a $10\,nM$ concentration in a TAE Mg^{++} buffer. The reaction has been realized in a humid chamber at 90°C for fifteen minutes to allow the separation of pBR322 strands and then cooled down to room temperature for two hours. Unbound molecules have been removed by successive rinsing procedures (SSC $2\times$ and $0.2\times$ solutions, 5 minutes each) which ensure high specificity for surface affinity reactions. Capturing oligonucleotides ($5' - SH - (CH_2)_6$gag ctc gga agc cca gta gta ggt$-3'$; MW $8570\,g/mole$; extinction coefficient: $269800\,l/mole\,cm$) have been provided to bind pBR322 strands by the use of of a 21-base long

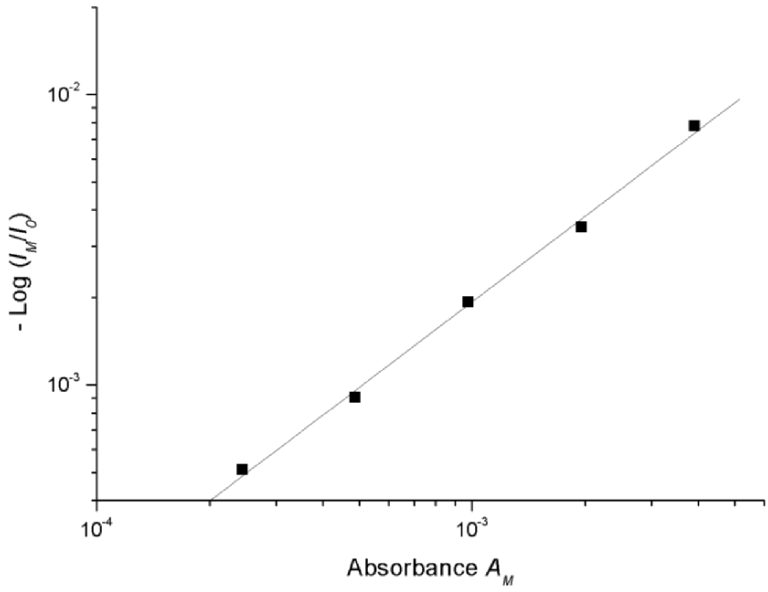

Fig. 4. Plot of the absorbance of molecular samples of low concentrations measured with the photodetector vs. their nominal value.

complementary sequence (acc tac tac tgg gct gct tcc in pBR322) and have been immobilized on sensing site by means of a standard procedure [33].

When target molecules were captured the sites exhibited higher absorbance and, consequently, a lower current was measured from the photodetectors (see in Fig. 5).

3.2 CMOS-Compatible Floating Gate Cells

This section presents an original approach based on the use of floating gate cells aiming at providing high-density arrays for integrated molecular detection and high flexibility in the choice of signal conditioning and processing strategies.

High-UV-sensitive floating gate cells have been exploited as devices to measure DNA molecular absorbance. In these memories the electrons can be injected into the floating gate by tunnel effect and can be completely or partially removed by a certain dose (intensity × time-interval) of UV light. A particular kind of cells, single-poly memories, have been selected because the UV sensitivity of their floating gate was enhanced by specific design choices. A schematic representation of single-poly cells is sketched in Fig. 6, where the main features of the design can be observed:

– the floating gate is the top conductive layer of the device and, in our test-chip, it was entirely exposed to the light (under the passivation oxide);
– the floating gate extends for a large portion of the surface of the cell (which measures $20\,\mu m^2$ for this generation). An advanced modeling and experimental results on the characteristics of these wafers have been already presented in [34].

The test-chips have been fabricated by STMicroelectronics–Italia in $0.25\,\mu m$ CMOS technology. It should be noticed that, although these memory cells are far from being state of the art, their dimensions are comparable to the minimum surface that microfabrication of molecular spots can achieve with the existing technology.

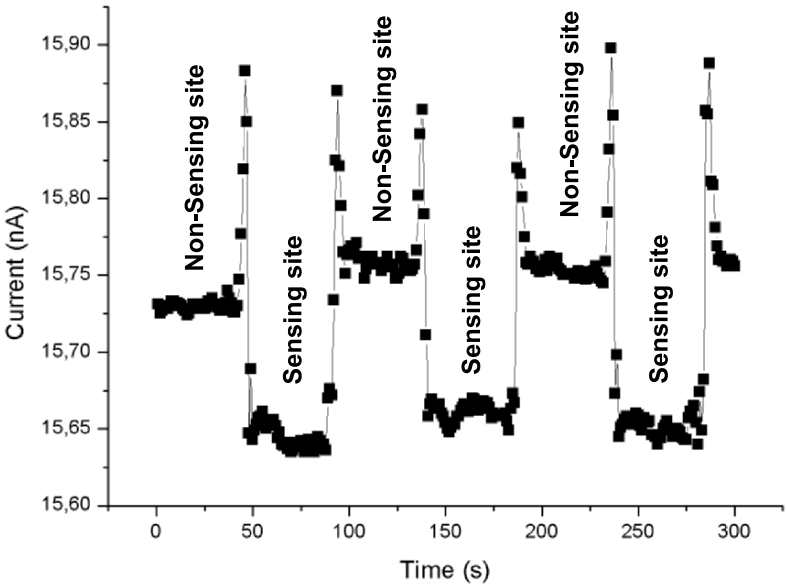

Fig. 5. Sites with only sensing probes (Non-Sensing sites) and sites with sensing probes and captured targets (Sensing Sites) have been aligned successively with a photodetector. The lamp drift was monitored with measurements of the white field and it causes variations in the order of $25\,pA$.

Method The erase-characteristic of the memory cell (the way the threshold voltage of the cell decreases with time during UV irradiation) depends on the intensity of the UV light with an exponential law [35]. The incident photons

impart energy to the electrons which have been stored in the floating gate during the programming process and excite them over the oxide energy barrier. The current due to the photo-excitation (I_{UV}) is a linear function of the light intensity at a given wavelength (Int_{UV}) and of the electric field E_{el}. When the control gate is at the same voltage than the substrate, the electric field across the oxide can be written as:

$$E_{el} = \frac{Q_{FG}}{C_{TOT} t_{ox}} \tag{5}$$

where Q_{FG} is the negative charge stored in the floating gate, C_{TOT} the total capacitance of the floating gate and t_{ox} the effective oxide thickness in the photo-excitation area.

The charge excited over the oxide has the following rate:

$$\frac{dQ_{FG}}{dt} = A_{eff} Int_{UV} \left(const1 \frac{Q_{FG}}{C_{TOT} t_{ox}} + const2 \right) \tag{6}$$

where A_{eff} is the effective area on the floating gate surface. $Const1$ and $const2$ are empirical constants depending on the light wavelength and on the silicon dioxide characteristics. Their ratio $const2/const1$ has the dimension of a field and is negligible with respect to E_{el}. Thus,

$$Q_{FG}(t) = Q_{FG}(0) e^{-\frac{Int_{UV} t}{\vartheta_0}} \tag{7}$$

where $Q_{FG}(0)$ is the charge at the beginning of the erase process and ϑ_0 equals $(A_{eff} const1)/(C_{TOT} t_{ox})$.

The erase characteristic can be written as follows:

$$Vth_{PR} - Vth_E(t) = (Vth_{PR} - Vth_{TOT\_E}) \cdot (1 - e^{-\frac{Int_{UV} t}{\vartheta_0}}) \tag{8}$$

where Vth_{PR} is the threshold voltage at the end of the programming process (beginning of the erasing process), Vth_{TOT_E} the threshold voltage corresponding to the floating gate trapping no electrons and $Vth_E(t)$ the threshold voltage after t seconds of UV light exposure.

For our purposes, let's consider that the UV light intensity can be attenuated by the presence of absorbing molecules on its path, thus affecting the erase characteristic. We demonstrated that floating gate cells may be used to analyze molecular samples (*i.e.* to provide a quantification or to detect the type of molecule) by observing their threshold after UV irradiation.

More particularly, the cell is programmed at a well-defined threshold voltage Vth_{PR} by injecting a corresponding amount of electrons in the floating gate. Then, the cell and the molecular sample are exposed to UV radiation during a certain time t. In the end, a different threshold voltage (Vth_E) – lower than Vth_{PR} – is reached. This threshold voltage depends on the container, solvent, absorbing biomolecules placed as filters on the UV-light path. The erase-characteristic has the following form:

$$Vth_{PR} - Vth_E(t) = (Vth_{PR} - Vth_{TOT\_E}) \cdot (1 - e^{-\frac{tInt_{UV}T}{\vartheta_0}}) \quad (9)$$

where T is the transmittance due to the absorbing effect of the molecular sample and of the container.

If Vth_{E1} and Vth_{E2} are the threshold voltages reached in case of two samples, their difference is related to the transmittances as follows:

$$Vth_{E1}(t) - Vth_{E2}(t) = (Vth_{PR} - Vth_{TOT\_E}) \cdot (e^{-\frac{tInt_{UV}T_2}{\theta_0}} - e^{-\frac{tInt_{UV}T_1}{\theta_0}}) \quad (10)$$

The analysis of the characteristics of a molecular sample is usually done with respect to a reference solution, which corresponds to the same solution in which molecules are diluted during measurements. The reference sample has a defined transmittance T_{REF} for which we can take into account at the denominator inside the constant τ_0. Correspondingly, the threshold voltage after a certain time of irradiation reaches $Vth_{REF}(t)$

For an certain molecular sample having a transmittance T_M:

$$Vth_E(t) - Vth_{REF}(t) = (Vth_{PR} - Vth_{TOT\_E}) \cdot (e^{-\frac{tInt_{UV}}{\tau_0}} - e^{-\frac{tInt_{UV}T_M}{\tau_0}}) \quad (11)$$

which directly links the threshold voltage of a sample to its transmittance and to its absorbance, as $A_M = -Log(T_M)$.

The difference between the exponentials will be maximum at a certain dose which should be evaluated for each setup.

Setup The source of UV radiation is a Xenon lamp, the distribution of which presents high emission values in the range of interest 250 to 270 nm. Though the lamp is controlled by a special circuit maintaining the supplied power constant ($100W$), radiation stability over long time periods is not guaranteed. That is why the radiation needs to be measured to compute the effective dose. This system is based on a photodiode the output current of which is amplified by an I/V converter and sampled by the use of an acquisition board equipped with 16-bit converters. The photodiode is placed directly after the UV filter needed to select the radiation range of interest and before the DNA sample container. Then a LabVIEW program controls the shutter and switches off the radiation once the dose has reached the desired value.

The cell characteristic is traced once the light source is masked by means of a HP4156 Semiconductor Parameter Analyzer (SPA) driven by the control PC. The threshold voltage is conventionally defined as the control gate polarization needed to obtain a drain current of $2\,\mu A$ when the drain is driven to $1\,V$ and source and bulk are grounded. Resolution in threshold voltage is $1\,mV$.

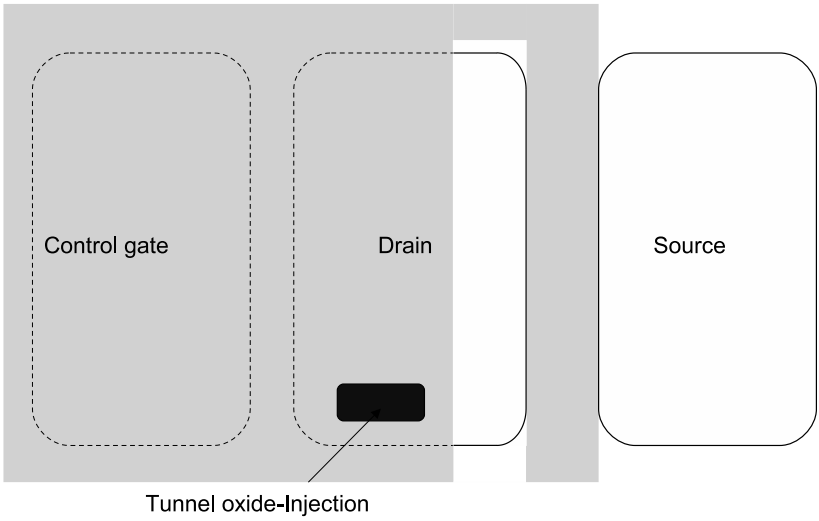

Fig. 6. Schematic top view of single-poly memory cells. The polysilicon floating gate extends for a large portion of the whole cell and it is exposed directly to the light under the silicon dioxide top passivation. The control gate is realized by means of a diffusion as source and drain and not by a second polysilicon layer.

Measurement of DNA hypochromic effect In our experiments, the reference sample (see Sect. 3.2) was a quartz container filled with $1.5\,ml$ buffer solution (TE $1\times$). So the optical path through the liquid sample was $1\,cm$ long. Two different forms of DNA molecule have been considered: single-stranded and double-stranded (two single strands zipped in a double helix). The total absorbance of two separate single strands is 30% bigger than that of the double helix form. This is known as hypochromic effect of DNA which is due to the fact that the interaction of the nucleotide bases with light changes when the strands are bound together.

The strands were 25 or 30 bases long. DNA molecular samples in the two forms have been analyzed in different concentrations by means of floating gate cells erase-characteristics (Fig. 7). On the x axis we reported the concentration of the nucleotide bases for each sample and on the y axis the threshold voltage at the time t of the erasing process. Each measurement is repeated 5 times and the standard deviation is indicated by the errors bars for each point (the latter cannot be easily seen on the plot as they measure $1\,mV$).

The two forms of the molecules are clearly distinguishable even for $1\,\mu M$ bases concentration, which means a resolution equaling the 30% on a 15×10^{-3} absorbance scale corresponding to the single-stranded sample. Such a behavior is comparable to that obtained with standard spectrophotometers [36]. Nevertheless, signal to noise ratio would be remarkably improved by an integrated setup.

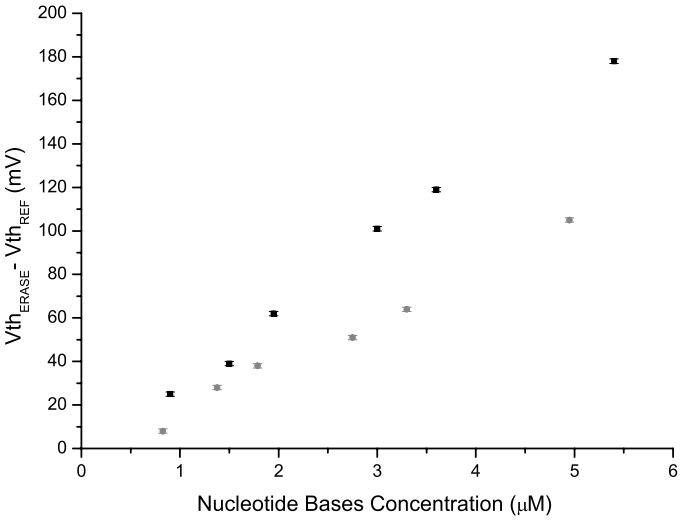

Fig. 7. Experimental plot and linear fit of the measurements of single-stranded (squares) and double-stranded (circles) DNA molecules for different concentrations.

4 Conclusions

Two silicon technologies aimed at the implementation of optical detectors for integrated molecular analysis tools have been selected and tested. The amorphous silicon devices have demonstrated high UV absorbance sensitivity down to 3×10^{-4}. They have also been employed to measure the presence of captured target molecules on a sensing site.

CMOS-compatible floating gate cells, suitable for high-parallel assays have been employed to detect molecular samples of different forms and concentrations. The erase-characteristics have been shown to follow a reproducible exponential law. Besides the cells have been able to detect the hypochromic effect of DNA down to 15×10^{-3} absorbance or at a concentration of $300\,nM$ short oligonucleotide strands.

References

1. Liu R H, Yang J, Lenigk R, Bonanno J, Grodzinski P, (2004) Anal. Chem., 76:1824 – 1831
2. Lagally E T, Medintz I, Mathies R A, (2001) Anal. Chem., 73:565 – 570
3. Lagally E T, Scherer J R, Blazej R G, Toriello N M, Diep B A, Ramchandani M, Sensabaugh G F, Riley L W, Mathies R A, (2004) Anal. Chem. 76:3162 – 3170
4. Kelly Ryan T, Woolley A T, (2005) Anal. Chem., 77(5):97A – 102A

5. Woolley A T, Sensabaugh G F, Mathies R A, (1997) Anal. Chem., 69:2181 – 2186
6. Shi Y, Simpson P C, Scherer J R, Wexler D, Skibola C, Smith M T, Mathies R A, (1999) Anal. Chem., 71:5354 – 5361
7. Terbrueggen R H, Chen Y-P, Duong H, Millan K M, Mucic R C, Olsen G T, Singhal P, Swami N, Wang H, Welch T W, Yowanto H, Yu C J, Blackburn G F, Kayyem J F, (2001) European Solid-State Devices and Research Conference, 1:119 – 121
8. Schienle M, Frey A, Hofmann F, Holzapfl B, Paulus C, Schindler-Bauer P, Thewes R, (2004) Solid-State Circuits Conference, Digest of Technical Papers, 1:220 – 524
9. Stagni Degli Esposti C, Guiducci C, Benini L, Riccò B, Carrara S, Samorì B, Paulus C, Schienle, Augustyniak M, Thewes R, (2006) Journal of Solid-State Circuits, 41(12):2956 – 2964
10. Wu G, Ram D, Hansen K M, Thundat T, Cote R J, Majumdar A, (2001) Nature Biotechnology, 19:856 – 860
11. Fritz J, Baller M K, Lang H P, Rothuizen H, Vettiger P, Meyer E, Guntherodt H J, Gerber C, Gimzewski J K, (2000) Science, 288:316 – 318
12. Lin V S-Y, Motesharei K, Dancil K, Sailor M J, (1997) Science, 278(5339):840 – 843
13. Prasad T, Colvin V, Mittleman D, (2003) Physical Review B, 67:165103-1 – 165103-7
14. Thrush E, Levi O, Cook L J, Deich J, Kurtz A, Smith S J, Moerner W E, Harris J S Jr, (2005) Sens. and Act. B, 105(2):393 - 399
15. Kamei T, Paegel B M, Scherer J R, Skelley A M, Street R A, Mathies R A, (2003) Anal. Chem., 75-20:5300 - 5305
16. Webster J R, Burns M A, Burke D T, Mastrangelo C H, (2001) Anal. Chem., 73-7:1622 - 1626
17. Nakanishi H, Nishimoto T, Arai A, Abe H, Kanai M, Fujiyama Y, Yoshida T, (2001) Anal. Chem., 22(2):230 - 234
18. Xu C, Li J, Wang Y, Cheng L, Lu Z, Chan M, (2005) IEEE Electron Device Letters, 26(4):240 - 242
19. Misiakos K, Kakabakos S E, Petrou P S, Ruf H H, (2004) Sens. and Act. B, 76(5):1366 - 1373
20. Fixe F, Chu V, Prazeres D M F, Conde J P, (2004) Anal. Chem., 32(9):e70
21. Thrush E , Levi O , Ha W, Wang K, Smith S J, Harris J S, (2006) Journal of Chromatography A, 1013:103 - 11
22. Romualdi C, Trevisan S, Celegato B, Costa G, Lanfranchi G, (2003) Nucl. Acids Res., 31(23):e149-1 — e149-8
23. Tinoco I, Sauer K, Wang J C, Puglisi J D (2001) Chemistry:Principles and Applications in Biological Sciences. Prentice Hall, New York.
24. Liu M, Jie L, (1999) J Phys. Chem. B, 103(51):11393 - 11397
25. Pei R, Cui X, Yang X, Wang E, (2001) Biomacromolecules, 2(2):463 - 468
26. Shi X, Sanedrin R J, Zhou F, (2002) J. Phys. Chem. B, 106(6):1173 - 1180
27. Kennedy G C, Matsuzaki H, Dong S, Liu W M, Huang J, Liu G, Su X, Cao M, Chen W, Zhang J, Liu W , Yang G, Di X, Ryder T, He Z, Surti U, Phillips M S, Boyce-Jacino M T, Fodor S PA, Jones K W, (2003) Nature Biotechnology, 10(10):1233 - 1237
28. Wang D, Urisman A, Liu Y, Springer M, Ksiazek T, Erdman D, Mardis E, Hickenbotham M, Magrini V, Eldred J, Latreille J, Wilson R, Ganem D, DeRisi J, (2003) PLoS Biology, 1(2):257260
29. Abruzzo L, Lee K, Fuller A, Silverman A, Keating M, Medeiros L, Coombes K, (2005) Biotechniques, 38(5):785 - 792

30. Conzone S D, Pantano C G, (2004) Materials Today, 7(33):20 - 26
31. Caputo D, de Cesare G, Irrera F, Tucci M, (1998) J. of Non-Cryst. Solids, 2:1316 – 1320
32. de Cesare G, Caputo D, Nascetti A, Guiducci C, Riccó B, (2006) Appl. Phys. Lett., 88: 083904-1 – 083904-3
33. Rogers Y, Jiang-Baucom P, Huang Z, Bogdanov V, Anderson S, Boyce-Jacino M T, (1999) Anal Biochem, 266(1):23 - 30
34. Lanzoni M, SuiiC J, Olivo P, Riccó B, (1993) IEEE Trans. on Electron Devices, 30(5):951 – 957
35. Katznelson R D, Frohman-Bentchkowsky D, (1980) IEEE Trans. on Elect. Dev., 27(9):1744 – 1752
36. http://www.biotek.com/products/docs/Nucleic_Acid_Quantitation_Tech_Note.pdf